Article

Design and Research of a Harvesting Actuator for *Camellia oleifera* Flowers during the Budding Period

Zechao Wu, Lijun Li *, Qing Zhao, Xin Guo and Jun Li

College of Mechanical and Electrical Engineering, Central South University of Forestry and Technology, Changsha 410004, China

* Correspondence: junlili1122@163.com

Abstract: The collection of *Camellia oleifera* flowers is a key foundation of *Camellia oleifera* flower pollen extraction. Due to the current problems of low efficiency, high labor intensity and the high cost of manual collection of *Camellia oleifera* flowers, a harvesting actuator was designed. By analyzing the inherent characteristics of the *Camellia oleifera* flower and the harvesting method, a harvesting structure using a combination of friction roller twisting harvesting and pipeline pneumatic conveying was designed. The geometric model of the *Camellia oleifera* flower was established and the motion analysis of the flower was carried out, which indicated that the *Camellia oleifera* flower would tend to a stable state for easy picking after entering the actuator. Using Automatic Dynamic Analysis of Mechanical Systems 2015 software (ADAMS, MSC. Software Corporation, Santa Ana, CA, USA) to simulate the process of *Camellia oleifera* flower picking, a mechanical analysis was performed in the contact plane to prove the theoretical feasibility of friction roller picking these flowers, and the main influencing factor was obtained as the speed of the friction roller. The test prototype for *Camellia oleifera* flower picking was built, and the picking experiment was implemented to study the effect of motor speed on the picking time of single *Camellia oleifera* flowers and the effect of the success rate of the flower picking. The test results show that when the motor speed is 400 r/min, the picking success rate is 96%, the picking time of a single flower is 1.2 s, and the speed of the machine collection of *Camellia oleifera* flowers is 2.3 times that of manual collection, which proves the realistic feasibility of this picking actuator. This paper provides an important reference and basis for the research and development of a flower harvesting actuator.

Keywords: *Camellia oleifera* flowers; harvesting actuator; picking mechanism; force analysis; picking experiment; efficiency

1. Introduction

Camellia oleifera is one of the unique woody oil crops in China and is an important economic crop with a planting area of about 4.85 million hectares. The fruiting rate and yield of *Camellia oleifera* can be improved by external intervention in the pollination of *Camellia oleifera* flowers [1,2]. At present, the external intervention pollination method is divided into two kinds: artificial intervention pollination and insect vector intervention pollination, and honeybee pollination is the main form of insect vector intervention pollination—but the galactose component in *Camellia oleifera* nectar and pollen is toxic to honeybees, which can easily lead to bee poisoning [3,4]. Manual intervention pollination is divided into two processes: pollen collection and stigma pollination, and the stigma pollination process can be carried out efficiently by machines such as mist sprayers and drones. Manual pollen collection requires the collection of a large number of *Camellia oleifera* flowers for pollen extraction, and the process is time-consuming, labor-intensive and inefficient, so collecting *Camellia oleifera* flowers has been a major problem for fruit farmers [5–7]. The collection of *Camellia oleifera* flowers for pollination has always been a method used by fruit farmers to increase production and income. *Camellia oleifera* flower picking, pollen

extraction and pollination has become mechanized, which is an inevitable trend of the benign development of the *Camellia oleifera* industry, of which picking is one of the most time-consuming and labor-intensive aspects; however, it is also the key and basis for pollen extraction and pollination, so reducing the cost of picking, reducing labor intensity, and achieving the mechanization of *Camellia oleifera* flower collection is imperative.

Research on flower harvesting actuators has been in a constant state of development. American researchers have developed a hops harvesting machines that uses roller picking and wind screening, and after continuous improvement, the mechanized picking of hops has now been achieved [8]. Willoughby, Solie and Whitney developed a chrysanthemum harvester using a combination of eccentric wheels and a comb knife for picking chrysanthemums in 2000, but the picking success rate was not high [9]. Dehkordi, Hanjani and Chegini developed a chrysanthemum picker in 2014 that uses a comb structure to pick chrysanthemums. The machine is simple in structure but the picking process causes a lot of damage to the plant [10]. Ravutov and Olimjonov developed a cotton harvesting machine using a combination of tooth combs and rollers in 2021 that is capable of picking cotton, but the large size of the machine makes it unsuitable for picking cotton grown in small areas [11]. Wang proposed the use of a robotic arm with a robotic hand to pick roses in 2014, which can pick roses, but the efficiency is too low [12]. Cao et al. developed a harvester for picking saffron silk using harvesting teeth in 2018, and it is highly efficient but also damaging to the plant [13]. Ji et al. developed a hand-pushed chrysanthemum harvester with high flexibility and high harvesting efficiency by using a comb combination cutting method in 2016, but the size was too small to be used for woody plant picking [14]. There are many types of machines, but none of them can harvest *Camellia oleifera* flowers effectively. Although there have been great breakthroughs in the research of flower harvesting machines, there is still no flower harvesting machine for the *Camellia oleifera* flower type [15–17]. In this paper, we analyze the inherent characteristics of *Camellia oleifera* flowers and their picking methods, design a harvesting actuator that can pick *Camellia oleifera* flowers, and conduct field tests.

2. Analysis of Inherent Characteristics of *Camellia oleifera* Flowers

To achieve the mechanized picking of *Camellia oleifera* flowers, we must first analyze the inherent and mechanical characteristics of *Camellia oleifera* flowers and determine the picking method before we can design the *Camellia oleifera* flowers harvesting actuator. The *Camellia oleifera* flower of the "Sanhua" variety, which is the most locally grown in Hunan Province, China, was selected for the analysis.

2.1. Biological Characteristics of Camellia oleifera Flowers

Camellia oleifera belongs to the economic forestry crops that flower and fruit during the same period, its growth is slow and growth cycle is long, it flowers in the autumn and winter of each year, and it fruits during the autumn and winter of the following year. The process of opening *Camellia oleifera* flowers goes through five periods: the budding period, initial opening, petal standing, petal falling and column withering. The single flower opening period is about seven days [18,19].

Camellia oleifera flowers grow at the end of branches in single growths or clusters. The shape and size of different flowering periods have notable differences, among which the budding period, blooming period and petal opening period are the harvesting periods of *Camellia oleifera* flowers. Statistics on the composition of the number of pickable *Camellia oleifera* flowers on the *Camellia oleifera* tree indicate that about 65% of the *Camellia oleifera* flowers are present during the budding period, so determining the object of picking for the budding period of *Camellia oleifera* flowers is significant. Figure 1 shows the *Camellia oleifera* flowers during the budding period.
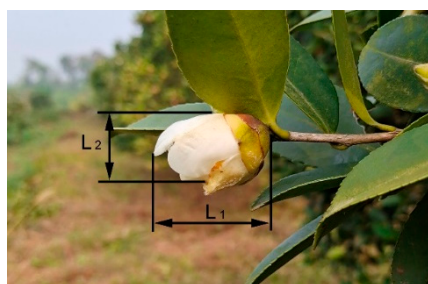
Figure 1. *Camellia oleifera* flower during the budding period.

Twenty *Camellia oleifera* trees that could be picked were randomly selected, two *Camellia oleifera* trees each constituted a group, and five *Camellia oleifera* flowers during the budding period were randomly selected from each tree as measurement samples—totaling 100 measurement samples. As shown in Figure 1, vernier calipers with specifications of 0 mm–100 mm and an accuracy of 0.01 mm were used to measure the maximum size L_2 and length L_1 of the *Camellia oleifera* flowers. The weight of the *Camellia oleifera* flowers was measured using a high-precision electronic scale with the specifications of 0 g–300 g and an accuracy of 0.01 g. The measurement results are shown in Figure 2.
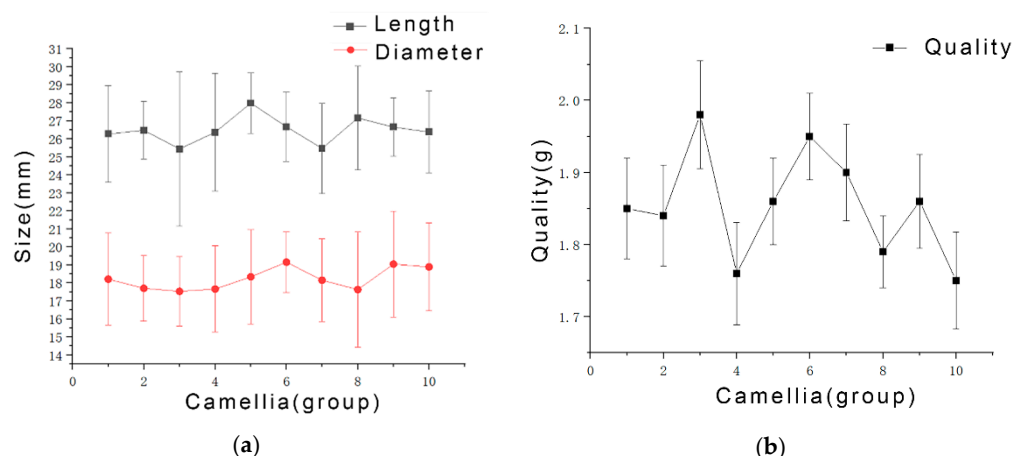

(**a**)

(**b**)

Figure 2. Measurement parameters of the *Camellia oleifera* flower. (**a**) *Camellia oleifera* flower size diagram. (**b**) *Camellia oleifera* flower mass diagram.

From Figure 2, the size and mass of the *Camellia oleifera* flowers in the budding period are shown. The average mass of *Camellia oleifera* flowers was 1.9 g, the average size was 18.3 mm, and the average length was 26.5 mm; these results were obtained statistically.

2.2. Mechanical Properties of Camellia oleifera Flowers

An analysis of the mechanical characteristics of *Camellia oleifera* flowers included the measurement of the tension force and torsional moment between the *Camellia oleifera* flowers and the flower stem and the measurement of the friction factor of the *Camellia oleifera* flowers. The dimensional model of the *Camellia oleifera* flowers was constructed according to the dimensions of the *Camellia oleifera* flowers and the measurement is drawn as shown in Figure 3.
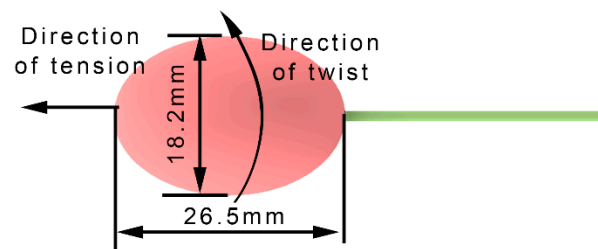
Figure 3. *Camellia oleifera* flower model.

Ten randomly selected *Camellia oleifera* trees that were available for picking were selected, and each tree was used in a group. From each tree, five *Camellia oleifera* flowers at the budding period were randomly selected for torsional moment detection—totaling 50 experimental samples—and five *Camellia oleifera* flowers at the budding period were randomly selected from each tree for positive tension force detection—totaling 50 experimental samples. The torsion force of the *Camellia oleifera* flower was measured by an HP-10 torsion tester, and the range of measurement was (0.004 N. m–1.000 N. m). The torsion tester was used to clamp the *Camellia oleifera* flower, twist the branch, and record the maximum torsion force when the *Camellia oleifera* flower was picked. Using the "three measures" pulling pressure meter to detect the situation of the *Camellia oleifera* flowers and the flower stalk, the instrument measurement range was (0.001 N–300 N), and the use of a string that tied up the *Camellia oleifera* flowers along the axial pulling helped record the maximum pulling force when picking. The measurement results are shown in Figure 4.
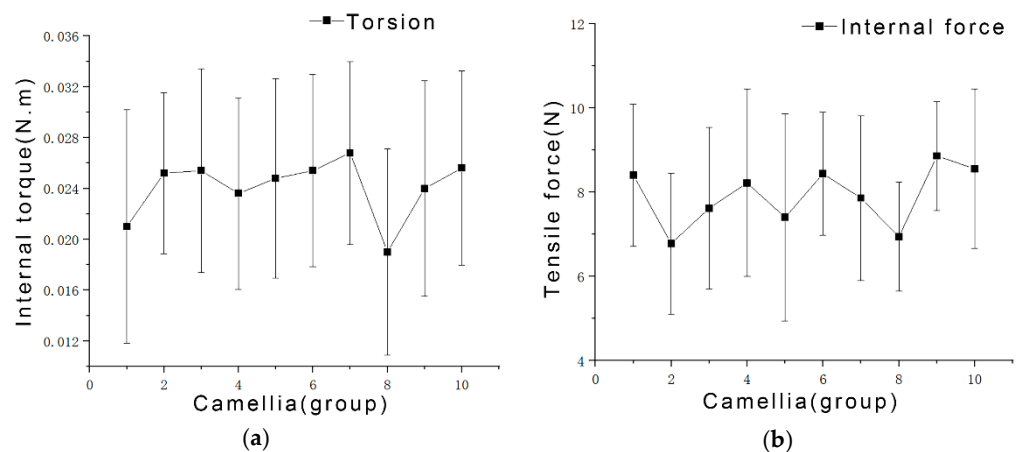

(a)

(b)

Figure 4. Binding force data of the *Camellia oleifera* flower samples. (**a**) *Camellia oleifera* flower torsion diagram. (**b**) *Camellia oleifera* flower internal force diagram.

From Figure 4, the torsional moment and tensile force of *Camellia oleifera* flowers during the budding period can be seen. The average value of the torsional moment of *Camellia oleifera* flowers was 0.02 N.m, as obtained from statistics, and the average value of the tensile force in the direction of the stem of *Camellia oleifera* flowers was 7.9 N.

Fifty *Camellia oleifera* flowers were picked and divided into ten groups equally, with five test samples in each group. The *Camellia oleifera* flowers were placed on the Rub Tester [20,21], the test values were recorded, and the friction coefficient of the *Camellia oleifera* flowers was calculated by Equation (1). The calculated values are shown in Figure 5.

$$\mu = \tan \delta \tag{1}$$

where:
μ—friction coefficient;
δ—tilt angle, $^{\circ}$.

From Figure 5, we can know the friction coefficient of *Camellia oleifera* flowers, and the average friction coefficient of the *Camellia oleifera* flowers and friction roller was calculated to be 0.68.
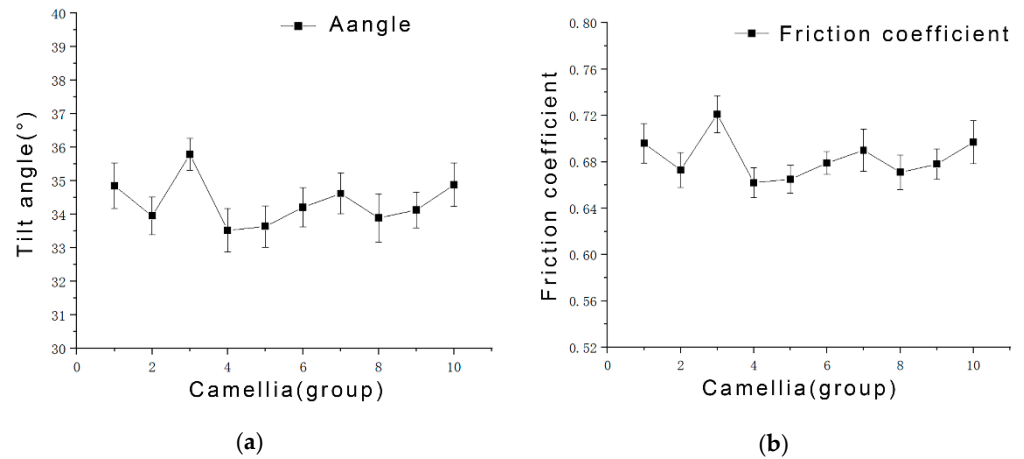

(**a**)

(**b**)

Figure 5. Tilt angle and friction coefficient data of the *Camellia oleifera* flower samples. (**a**) Experimental tilt angle of *Camellia oleifera* flower. (**b**) *Camellia oleifera* flower friction coefficient.

3. Structural Design and Operating Principle

3.1. Structure Composition

The manual hand picking of *Camellia oleifera* flowers is divided into two steps: picking and collecting. The *Camellia oleifera* flowers are picked by holding the flowers with the fingers and twisting them with the wrist. The picked *Camellia oleifera* flowers will be placed into the collection bag. This work process will be repeated until the collection bag is full [22,23]. According to the inherent characteristics of *Camellia oleifera* flowers, we designed a twist picking device to pick *Camellia oleifera* flowers. The shape of the picking mouth was designed to be V-shaped to accommodate the picking of different sizes of *Camellia oleifera* flowers. The structural model of the actuator was created using Autodesk Inventor Professional software (Inventor, Autodesk Inc. San Rafael, CA, USA), as shown in Figure 6.

(**a**)

(**b**)
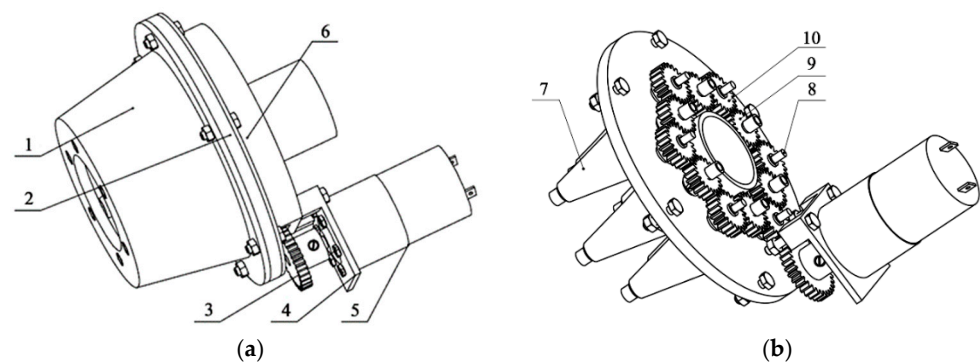
Figure 6. Schematic diagram of the structure of the *Camellia oleifera* flower harvesting actuator. (**a**) Harvesting actuator external structure diagram. (**b**) Harvesting actuator internal structure diagram. 1 V-enclosure, 2 Center frame, 3 Motor gear, 4 Motor frame, 5 Motor, 6 Endcap, 7 Friction roller, 8 Transmission gear shaft, 9 Friction roller gear, 10 Transmission gear.

The *Camellia oleifera* flower harvesting actuator has a simple structure and uses a gear transmission to ensure stability during the process of movement. The opening diameter of the V-shaped housing is 50 mm, the diameter at the exit of the central frame is 35 mm, the length of the friction roller is 50 mm, the diameter of the large end is 30 mm, and the

diameter of the small end is 10 mm. A spur gear drive of module 1 is used, the ratio of the friction roller gear to the drive gear is 1:1, and the ratio of the motor gear to the drive gear is 1:2. The number of friction rollers in the harvesting actuator is six and they are evenly distributed around the central axis, which ensures the wrapping of the friction rollers for the *Camellia oleifera* flowers and increases the contact area of the *Camellia oleifera* flowers in the harvesting actuator, as well as resulting in a better picking effect. The surface of the friction roller is designed with a threaded strip, which can guide the *Camellia oleifera* flower to move in the direction of the exit when twisting, thereby increasing the feasibility of picking and improving the picking efficiency [24,25]. Compared to the repetitive mechanical movement in manual picking, when using end-effector picking, a friction roller twist picking combined with pipeline transportation is used to combine picking and collecting into one, thereby improving labor intensity while increasing the picking efficiency.

3.2. Operating Principle

During the working process, the *Camellia oleifera* flowers enter into the V-shape cover, and different sizes of *Camellia oleifera* flowers go in at different depths to be able to ensure that they can all touch the friction roller. A motor power supply is used to drive the motor gear to rotate, and the motor gear drives the transmission gear to rotate around the transmission gear shaft, thereby transferring the force to the friction roller gear; subsequently, the friction roller gear drives the friction roller to rotate in the same direction. The *Camellia oleifera* flowers happen to rotate downward until they are picked off. After the *Camellia oleifera* flowers are picked, they are transported to the collection box by the pneumatic conveying system and the picking is completed. The *Camellia oleifera* flower picking actuator is a rigid structure that will cause damage to the petals of the *Camellia oleifera* flowers during the picking process. The function of the petals is to protect the stamens, so no damage will be caused to the stamens. The purpose of picking is to collect the stamens, so the rigid structure meets the needs of picking.

4. Research on *Camellia oleifera* Flower Picking

4.1. Analysis of Camellia oleifera Flower Posture

The *Camellia oleifera* flowers will enter the actuator in different positions, and the picking state of the *Camellia oleifera* flowers inside the actuator will be determined through motion analysis [26–28].

4.1.1. Geometric Model Analysis of *Camellia oleifera* Flowers

According to the measured geometrical parameters of the *Camellia oleifera* flower, the *Camellia oleifera* flower of the "Sanhua" variety is ellipsoidal during the budding period—the parameters are simplified for the theoretical calculation and analysis—and the *Camellia oleifera* flower is simplified to an ellipsoidal model [29,30]. A spatial coordinate system (*Oxyz*) is established, where the coordinate origin *O* coincides with the geometric center. The schematic diagram of the three-dimensional coordinates is shown in Figure 7.

The mathematical expressions of the *Camellia oleifera* flower model are established according to Figure 7.

$$\frac{x^2}{Lx^2} + \frac{y^2}{Ly^2} + \frac{z^2}{Lz^2} = 1 \tag{2}$$

where:
Lz—Length in Z-axis, mm;
Ly—Length in Y-axis, mm;
Lx—Length in X-axis, mm.

When the object is rotating around the Z-axis, V is the model volume, and the change in the moment of inertia of rotation is shown in Equation (3).
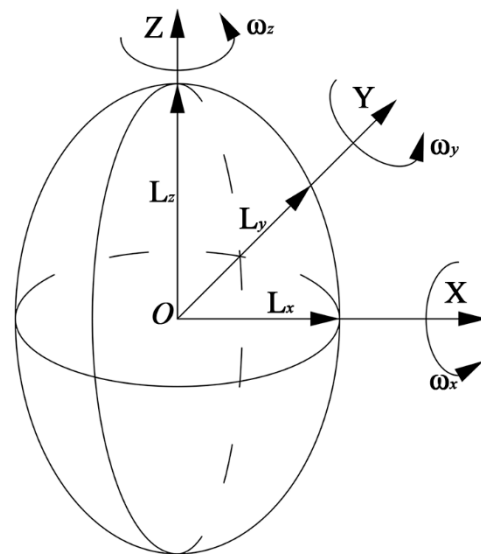
Figure 7. Schematic diagram of the three-dimensional coordinates of *Camellia oleifera* flower.

$$J_z = \iiint\limits_{V} \left(x^2 + y^2 \right) \rho \mathrm{d}v \tag{3}$$

Equation (3) is solved as a generalized spherical coordinate transformation to obtain the moment of inertia of the ellipsoid around the Z-axis (4).

$$J_z = \frac{1}{5} m \left(\mathrm{L}y^2 + \mathrm{L}x^2 \right) \tag{4}$$

Similarly, the moment of inertia of the ellipsoid around the X-axis and Y-axis is inferred as Equations (5) and (6), respectively.

$$J_x = \frac{1}{5} m \left(\mathrm{L}y^2 + \mathrm{L}z^2 \right) \tag{5}$$

$$J_y = \frac{1}{5} m \left(\mathrm{L}x^2 + \mathrm{L}z^2 \right) \tag{6}$$

where, J_x, J_y, and J_z are the moments of inertia of the *Camellia oleifera* flower around the X-, Y-, and Z-axis respectively, unit kg·m^2; and m is the mass of the *Camellia oleifera* flower in kg.

4.1.2. Analysis of the Movement of *Camellia oleifera* Flowers

When the *Camellia oleifera* flowers enter into the harvesting actuator for picking, they will have different postures. The friction roller set is V-shaped and gradually contracts from the opening inward, while the *Camellia oleifera* flower also changes its attitude with the roller. Due to the difference in inertia of the spindle rotation in the three directions of the *Camellia oleifera* flower, the *Camellia oleifera* flowers grow at the end of the flowering branch of the *Camellia oleifera* fruit tree. The branch itself has a large deflection deformation, and ideally the *Camellia oleifera* flower is not affected by the flowering branch. Using this information, the angular momentum equations of *Camellia oleifera* flowers are constructed [31–34].

$$\frac{d\vec{J}}{dt} = \vec{M} \tag{7}$$

The angular momentum equation is listed in the spatial coordinate system as shown in Equation (7). The solution for Equation (7) yields the Euler equation for the motion of the *Camellia oleifera* flower, as shown in Equation (8).

$$\begin{cases} J_x\dot{\omega}_x - (J_z - J_y)\omega_y\omega_z = M_x \\ J_y\dot{\omega}_y - (J_x - J_z)\omega_z\omega_x = M_y \\ J_z\dot{\omega}_z - (J_y - J_x)\omega_x\omega_y = M_z \end{cases} \tag{8}$$

where:

ω_x—Angular velocity of *Camellia oleifera* flower around X-axis, rad/s;

ω_y—Angular velocity of *Camellia oleifera* flower around Y-axis, rad/s;

ω_z—Angular velocity of *Camellia oleifera* flower around Z-axis, rad/s;

M_x is the moment of $\vec{M}$ on the X-axis, N.m;

M_y is the moment of $\vec{M}$ on the Y-axis, N.m;

M_z is the moment of $\vec{M}$ on the Z-axis, N.m.

By assuming that the *Camellia oleifera* flower is an equivalent rigid body, during the process of rotation, no deformation will occur in the axis of rotation, which is the Z-axis that deviates from the main axis of inertia; furthermore, ω_x and $\omega_y^{[OBJ]}$ are $\omega_z^{[OBJ]}$, which, at this time, does not receive interference from the external moments $M_x^{[OBJ]}M_y^{[OBJ]}$, and $M_z^{[OBJ]}$—whose value is 0. By simplifying Equation (8) to obtain the Euler equation of motion at this time, Equation (9) is obtained, as shown below.

$$\begin{cases} J_x\dot{\omega}_x = (J_y - J_z)\omega_y\omega_z \\ J_y\dot{\omega}_y = (J_z - J_x)\omega_z\omega_x \\ J_z\dot{\omega}_z = (J_x - J_y)\omega_x\omega_y \end{cases} \tag{9}$$

Based on the fact that ω_x and are much smaller than ω_z, we can obtain Equation (10) by simplifying Equation (9).

$$\begin{cases} \ddot{\omega}_x + \left[\dfrac{(J_z-J_y)(J_z-J_x)}{J_yJ_x}\omega_z^2\right]\omega_x = 0 \\ \ddot{\omega}_y + \left[\dfrac{(J_z-J_x)(J_z-J_y)}{J_yJ_x}\omega_z^2\right]\omega_y = 0 \end{cases} \tag{10}$$

The stability of the *Camellia oleifera* flower according to Formula (10) is determined as follows: When $J_z > J_y$, $J_z > J_x$ or $J_z < J_y$, $J_z < J_x$, $\omega_x\omega_y$ has an oscillatory solution and the system tends to be stable; when $J_x > J_z > J_y$ or $J_x < J_z < J_y$, $\omega_x\omega_y$ has an exponential growth solution and the system is unstable [35–38]. According to the geometric model calculation of *Camellia oleifera* flowers and Equations (4)–(6), we can get $J_z < J_y$, $J_z < J_x$. Therefore, under ideal conditions, after entering the system, the *Camellia oleifera* flowers will eventually tend to rotate around the central axis to achieve the most ideal picking posture, which provides a theoretical basis for *Camellia oleifera* flower picking analysis.

4.2. Force Analysis of Camellia oleifera Flower Picking

The *Camellia oleifera* flower picking process uses friction rollers to transmit force and a twisting method is used to pick the *Camellia oleifera* flowers. Through the proposed *Camellia oleifera* flower picking scheme, a three-dimensional model of the *Camellia oleifera* flower picking process is established [39–41]. The drawn three-dimensional model is imported into Automatic Dynamic Analysis of Mechanical Systems 2015 software (ADAMS, MSC. Software Corporation, Santa Ana, CA, USA) to constrain it, and the constraints are shown in Figure 8.

Since the friction rollers were evenly distributed around the *Camellia oleifera* flowers with the same structure, the friction rollers were subjected to the same constraints, so a set of constraints was selected for setting. The corresponding constraints were added according to the motion relationship and force between the *Camellia oleifera* flowers and the friction roller. The constraints are shown in Table 1.
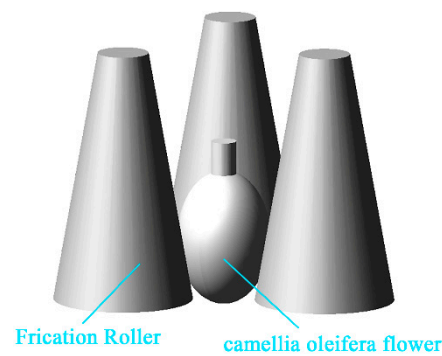
Figure 8. Picking simulation model.

Table 1. Model constraints used in the study.

Number	Constraint	Connection Components
1	Revolute	Friction roller and ground
2	Contact force	Friction roller and *Camellia oleifera* flower
3	Sliding pair	*Camellia oleifera* flower and the ground
4	Revolute	*Camellia oleifera* flower and the ground

After adding the constraints, the degree of freedom of the transmission mechanism is 1, so the mechanism can be driven by a single power, and the modify torque is 1, which is set as the driving torque on the friction roller with a torque value of 0.2 N.m. The bonding force between the *Camellia oleifera* flower and the flower stem is modified for torque 2, and the function of torque 2 is defined as IF(.MODEL_ 1.PAPT_MEA_1-0.1:−0.02, −0.02,0). When the angular velocity is less than or equal to 0.1 rad/s, the value of torque 2 is −0.02 N.m. When the angular velocity is greater than 0.1 rad/s, torque 2 becomes 0 N.m. By adding the friction coefficient 0.68 and quality 1.85 g to the friction constraint condition, the simulation time is set to 0.5 s and the simulation analysis is carried out. The simulation results of the torque variation of the *Camellia oleifera* flower are shown in Figure 9.
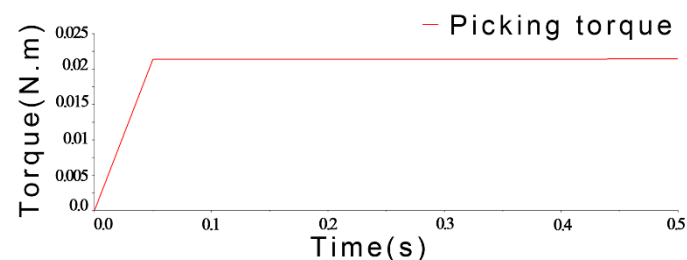

Figure 9. *Camellia oleifera* flower torque variation curve.

According to the change in the curve in the figure, it can be seen that the friction roller drives the *Camellia oleifera* flower in the process of rotation, and the torque gradually increases and then tends to stabilize, and after stabilization, the *Camellia oleifera* flower rotates and is only subject to the picking torque, and then the picking process is completed. In the Automatic Dynamic Analysis of Mechanical Systems 2015 software (ADAMS, MSC. Software Corporation, Santa Ana, CA, USA) simulation of the picking process, the *Camellia oleifera* flower can be divided into three periods from the beginning to the end of picking, as shown in Figure 10.
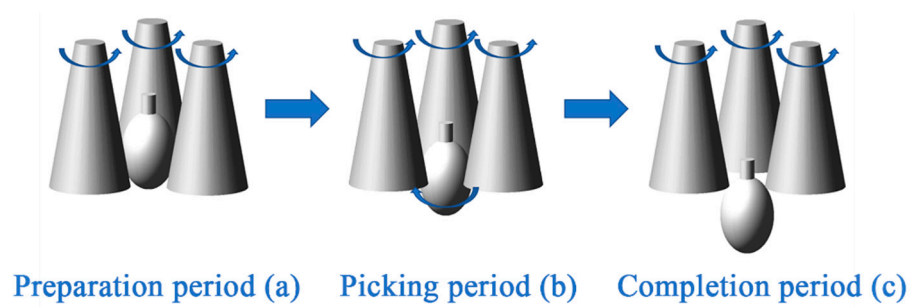
Preparation period (a)   Picking period (b)   Completion period (c)

Figure 10. Simulated picking process of a *Camellia oleifera* flower by the picking unit.

As shown in Figure 10, the rotation of the friction roller drives the rotation of the *Camellia oleifera* flowers after the rotation, and finally the *Camellia oleifera* flowers are successfully picked off. In the process of picking, the *Camellia oleifera* flower starts to stabilize in period (a). The friction roller starts to rotate and the *Camellia oleifera* flower has a relative rotation trend and reaches period (b). Gradually, the *Camellia oleifera* flower picking is completed in order to reach period (c). The tangential force on the surface of the *Camellia oleifera* flower for period (b) is the maximum static friction, and the contact surface of the tangent face for period (b) is shown in the contact model force sketch in Figure 11.
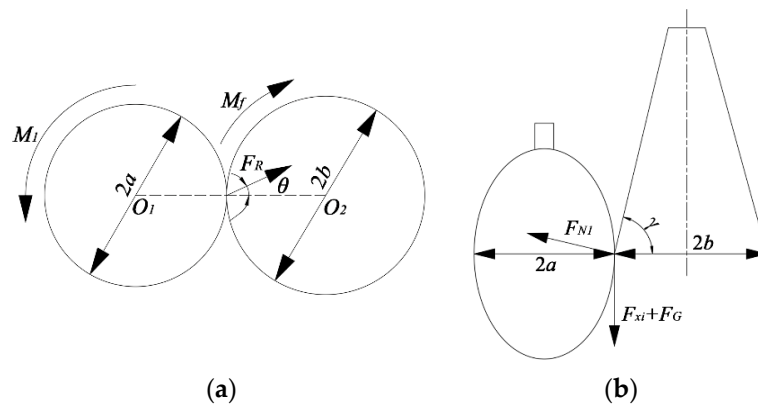

(a)   (b)

Figure 11. Contact surface model of the flower (**left**) and the friction roller (**right**). (**a**) Horizontal cut force. (**b**) Vertical cut force.

In Figure 11, the diameter of the *Camellia oleifera* flower is denoted as 2a, and the center of the circle is o_1; the diameter of the fri o_2o_2 From Figure 11, we can know the force situation of the *Camellia oleifera* flower during picking; the *Camellia oleifera* flower is in a steady state and has a tendency to move relative to the friction roller. By establishing the coordinate system with the X-direction as the horizontal direction and the Y-direction as the vertical direction, the forces can be listed in Equation (11).

$$\begin{cases} F_{Nx} = F_{N1} \sin \gamma \\ F_{Ny} = F_{N1} \cos \gamma - F_{xi} - F_G = 0 \end{cases} \tag{11}$$

where:
γ—Tilt angle of friction roller, °;
F_{N1}—The pressure generated by the friction roller on the *Camellia oleifera* flower, N;
F_{xi}—Sucking power of transport pipeline for *Camellia oleifera* flowers, N;
F_G—*Camellia oleifera* flower gravity, N;
F_{Nx}—Friction roller in *Camellia oleifera* flower x-axis, N.
Equation (12) on F_{Nx} is obtained by simplifying Equation (11).

$$F_{Nx} = (F_{xi} + F_G) \tan \gamma \tag{12}$$

The magnitude of the force exerted by the friction roller on the *Camellia oleifera* flower in the X-axis direction is obtained from Equation (12). Based on force diagram a, Static Equation (13) can be listed.

$$\begin{cases} M_1 + aF_R \sin\theta = M_f \\ F_{NA} = F_R \cos\theta \end{cases} \tag{13}$$

where:

M_f—*Camellia oleifera* flower resistance moment, N. m;
F_R—Frictional total reaction force, N;
M_1—Friction roller torsion moment, N. m;
θ—Friction angle, °;
F_{NA}—*Camellia oleifera* flower pressure, N.

Where F_{NA} is equal to the value of F_{Nx}. Furthermore, Equation (14) is obtained by analyzing the simplification of Equations (12) and (13).

$$M_f = M_1 + a(F_{xi} + F_G) \tan\gamma \tan\theta \tag{14}$$

At the time of contact, the friction roller cut surface is a uniform thin disc shape according to the rotational moment of inertia formula (15), which can be used to obtain the rotational moment M_1.

$$M_1 = J\alpha \tag{15}$$

where:

J—Friction roller rotational moments of inertia, Kg.m^2;
α—Friction roller Angular acceleration, rad/s^2.

The parameters of the friction roller are substituted into Equation (15) to obtain Equation (16).

$$\begin{cases} J = \frac{1}{2}mr^2 \\ \alpha = \frac{n\pi}{30t} \end{cases} \tag{16}$$

where:

m—Cut surface quality, g;
r—Cut surface radius, mm;
n—Friction roller rotation speed, r/min;

By simplifying Equations (14)–(16), torque Equation (17) can be obtained.

$$M_f = k\left[\frac{ma^2 n\pi}{60t} + a(F_{xi} + F_G) \tan\gamma \tan\theta\right] \tag{17}$$

In Equation (17), k denotes the number of friction rollers. From Equation (17), the factors affecting the magnitude of the torque of the friction rollers for performing the torsional picking process can be obtained. The radius of the friction roller, inclination angle, rotational speed and the number of friction rollers are the main factors that affect the torque. When the size of the *Camellia oleifera* flower is determined, the number of friction rollers around the *Camellia oleifera* flower has a correlation with the size, as shown in Figure 12.
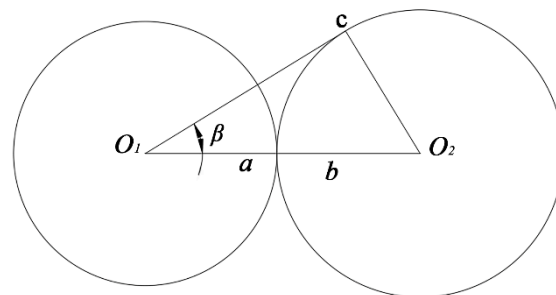

Figure 12. Friction roller distribution relationship.

From Figure 12, the relationship between the number of friction rollers and the diameter of the friction rollers is obtained as Equation (18).

$$b = \frac{a}{(1 - \sin\beta)} - a \tag{18}$$

In Equation (18), the value of β ranges from (0–60] degrees and the number of friction rollers is at least 3. In the design of the friction rollers, the number of friction rollers, rotational speed and inclination angle are the main variables, and it can be seen from Equation (17) and Equation (18) that by increasing the radius, inclination angle, rotational speed and the number of friction rollers, sufficient torque can be provided to pick the *Camellia oleifera* flowers. Therefore, the *Camellia oleifera* flowers can be picked smoothly by using the friction roller picking method, and efficient picking can be achieved by adjusting the friction roller rotational speed.

5. Prototype Performance Test and Analysis

5.1. Test Introduction

According to the design plan of the harvesting actuator for *Camellia oleifera* flowers, a test prototype of the harvesting actuator was made and mounted on a portable suction machine. The dimensions of the collection box were designed to be 460 mm * 260 mm * 500 mm, with a pipe length of 1000 mm and a pipe diameter of 650 mm. The suction conveying consisted of closed smooth pipes with no mechanical moving parts, which ensured smooth and efficient conveying of harvested *Camellia oleifera* flowers to the collection box. There was a portable lithium battery installed on the outer bottom of the collection box, with a battery capacity of 20 A and a voltage of 24 V, and a maximum continuous working time of about 5 h, which could complete the flower picking of about 90 *Camellia oleifera* trees. The speed of the motor was adjusted by the knob and the specific speed value was obtained by calculating the speed duty cycle on the digital motor governor. A picking test was conducted by the experimenter to test the working performance of the actuator, and the test prototype is shown in Figure 13.
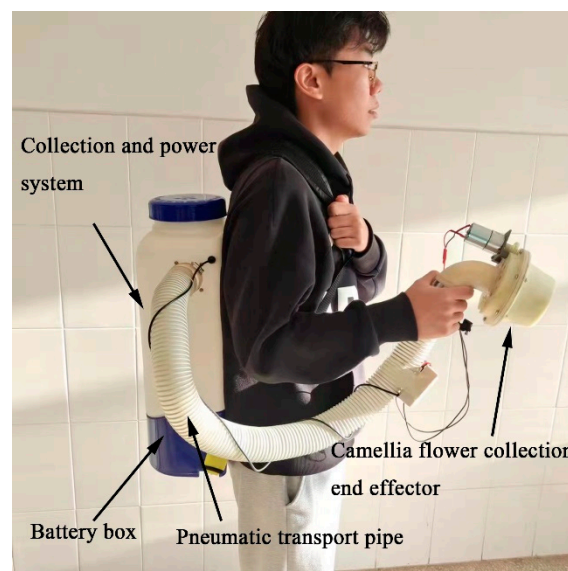
Figure 13. Prototype harvesting system for the *Camellia oleifera* flowers.

5.2. Materials and Methods

Through theoretical analysis, it was concluded that the friction roller motor speed was the main factor that affects the picking of *Camellia oleifera* flowers. It was found that the minimum motor speed of the harvesting actuator for picking *Camellia oleifera* flowers was 200 r/min. The friction roller picking process showed obvious vibrations when the motor

speed exceeded 400 r/min, and when the motor speed exceeded 500 r/min, the harvesting actuator made a strange noise and was not suitable for further picking.

With the motor speed as the influencing factor, a picking test was designed with the harvesting time and harvesting success rate of *Camellia oleifera* flowers as the index. During the experiment, the static pressure of the airflow was about −2100 Pa, which was able to transport the *Camellia oleifera* flowers smoothly and provide about 0.53 N of suction force for picking. In this regard, the single harvesting time was the time when the *Camellia oleifera* flower was aligned with the outer end of the end-effector and had not yet entered the inner part of the actuator, and ended when the *Camellia oleifera* flower entered the collection box. When the *Camellia oleifera* pistils were picked into the collection box, this was considered a successful picking. The ratio of the number of successfully picked samples to the total number of samples in the picked sample group was defined as the picking success rate. When only the petals were picked while the stamens remained on the flower stems, it was defined as a failed picking.

5.3. Results and Discussion

In the test, the picking motor speed was regulated (200–500 rpm) and divided into 13 groups. The test site was selected from the experimental base of *Camellia oleifera* in Wangcheng, Changsha, Hunan, and the test variety was selected from the "Sanhua" *Camellia oleifera* variety. *Camellia oleifera* flowers with a diameter range of 15–20 mm were used as experimental samples, with a diameter gradient of 0.5 mm, and 50 experimental samples were taken at each speed—for a total of 650 samples. The harvesting time and harvesting success rate of *Camellia oleifera* flowers were counted. These data were compiled to obtain the average harvest time of single flowers and the average harvest success rate. The standard deviation of the single flower picking time was obtained by calculating the picking time, and the stability of the picking process was reflected by the standard deviation of the single flower harvest time. The results are shown in Table 2. In order to clearly express the moment of picking, the handheld method was used to take pictures, and it was not necessary to hold the *Camellia oleifera* flowers during normal work. The picking process is shown in Figure 14.

Table 2. Harvest time and harvest success of the prototype harvesting system for the *Camellia oleifera* flowers.

Motor Speed (r/min)	Average Harvest Time of a Single Flower (s)	Average Harvesting Success Rate (%)
200	1.62 ± 0.10	90
225	1.55 ± 0.07	90
250	1.41 ± 0.08	92
275	1.42 ± 0.07	92
300	1.39 ± 0.06	94
325	1.37 ± 0.07	94
350	1.31 ± 0.07	94
375	1.25 ± 0.06	96
400	1.21 ± 0.06	96
425	1.31 ± 0.09	90
450	1.30 ± 0.16	96
475	1.35 ± 0.25	80
500	1.50 ± 0.29	82

As can be seen from Table 2, when the motor speed was within (200–400 rpm), the motor speed was positively correlated with the harvesting success rate, and the motor speed was inversely correlated with the harvesting time. When the motor speed exceeded 400 r/m, the standard deviation of the single flower harvest time increased and the harvesting success rate fluctuated. To avoid changes to the test, the motor speed was adjusted within (410 r/min–500 r/min), and the trees were divided into 10 groups for testing; the *Camellia*

oleifera flower standard was unchanged, 50 samples were picked from each group for each speed, and the total number of samples was 500. The time and success rate of *Camellia oleifera* flower picking were counted, and the experimental results are shown in Table 3.

Figure 14. Experimental process diagram of the prototype harvesting system for the *Camellia oleifera* flowers. (**a**) Find flowers. (**b**) Flower entry actuator. (**c**) Start picking. (**d**) Picking is complete.

Table 3. Various picking indices at 410 r/min–500 r/min motor speed.

Motor Speed (r/min)	Average Harvest Time of a Single Flower (s)	Average Harvesting Success Rate (%)
410	1.32 ± 0.10	88
420	1.31 ± 0.16	90
430	1.42 ± 0.15	80
440	1.44 ± 0.12	76
450	1.30 ± 0.16	96
460	1.46 ± 0.15	82
470	1.35 ± 0.27	80
480	1.32 ± 0.28	76
490	1.48 ± 0.25	80
500	1.50 ± 0.29	82

According to Table 3, when the motor speed is adjusted within (410–500 rpm), the harvesting time and harvesting success rate are irregularly distributed. In this speed range, the harvesting success rate fluctuates too much, the standard deviation of the single flower harvest time is large, the picking time is unstable, the friction roller vibrates significantly,

the drive gear wears significantly, and the actuator stability is poor. Given this, this speed is not suitable for picking operations, and the maximum speed should be controlled to 400 r/min during the picking process. Therefore, when the motor speed is 400 r/min, which is the optimal speed, the shortest harvesting time can reach 1.2 s, and the harvesting success rate is 96%. Using the picking actuator to pick *Camellia oleifera* flowers will cause damage to the petals, but will not affect the internal anthers, which can ensure the integrity of the *Camellia oleifera* flowers—and the *Camellia oleifera* flowers obtained from the picking will all meet the picking requirements.

Using the *Camellia oleifera* flower harvesting machine to pick *Camellia oleifera* flowers, 1.98 kg of *Camellia oleifera* flowers can be collected in one hour, and 0.85 kg of *Camellia oleifera* flowers can be collected in one hour by manual picking, proving that the speed of the machine collection of *Camellia oleifera* flowers is 2.3 times that of the manual collection of *Camellia oleifera* flowers. In addition, it was found that the speed of manual collection became significantly slower with an increase in time, while the deceleration effect of using the picking machine to collect *Camellia oleifera* flowers was not obvious. Therefore, the advantage of using the picker to pick *Camellia oleifera* flowers would be more obvious in the long time collection work, and the efficiency of collecting with the picker was significantly higher than that of manual collection.

5.4. Test Conclusion

During the picking process, picking failure will damage the *Camellia oleifera* flowers. The test shows that when the motor speed is less than 200 r/min, the *Camellia oleifera* flowers cannot be picked successfully, and at this time the twisting force applied by the friction roller on the *Camellia oleifera* petals is greater than the bonding force between the petals and the connecting part of the pistil; however, it is less than the bonding force between the flower and the flower stem, so the picking fails. When the motor speed is at 200–400 rpm, the motor speed is positively proportional to the harvesting success rate and inversely proportional to the harvesting time. When the motor speed exceeds 400 r/min, the harvesting actuator vibrates, and the *Camellia oleifera* flowers collide violently with the friction roller, which easily leads to the petals falling off; furthermore, at this time, the harvesting time and the harvesting success rate change irregularly, and the picking stability is poor, which is not suitable for picking. Therefore, the picking speed is set to 400 r/min, the harvesting success rate is 96%, the harvesting time for a single flower is 1.2 s, the standard deviation of the single flower harvesting time is 0.06, the picking effect is the best, and the picking time is the most stable. This end-effector, which is positioned and manually operated by the human eye, ensures flexibility in harvesting while increasing productivity, improving labor intensity, and ensuring that pollen is harvested at high pollen activity stages.

6. Conclusions

The harvesting of *Camellia oleifera* flowers plays an important role in the pollination process of *Camellia oleifera* flowers. By analyzing the inherent characteristics of *Camellia oleifera* flowers and imitating the working principle of manual harvesting of *Camellia oleifera* flowers, a new picking method was proposed and an end-effector using friction rollers for twisting harvesting was designed. This end-effector combined picking and collecting functions to improve the picking efficiency and to reduce labor costs, thereby solving the current situation that no machinery is available for *Camellia oleifera* flower picking. It is the first actuator among current flower harvesting actuators that can be used for *Camellia oleifera* flower picking, and the feasibility of this research has been proven through theoretical analysis and experimental verification.

The kinematic analysis calculated that the *Camellia oleifera* flower, after entering the end-effector, would tend to a stable state where the actuator and the axis of the *Camellia oleifera* flower coincided to reach a suitable attitude for the harvesting of the *Camellia oleifera* flower. The mechanical analysis of the picking process was carried out, and it was obtained

that the number of rollers, the rotational speed and the inclination angle of the rollers were the main factors affecting the picking when the *Camellia oleifera* flower was picked, among which the rotational speed was the main factor. The test results show that when the motor speed is in the range of (200–400 rpm), the motor speed has a positive relationship with the harvesting success rate and the motor speed has an inverse relationship with the harvesting time. Given this, a motor speed of 400 r/min is the best picking speed for this actuator, as is evidenced by a harvesting success rate of 96% and a single flower harvesting time of 1.2 s. Moreover, the speed of the machine collection of *Camellia oleifera* flowers is 2.3 times that of manual collection. This study proved the feasibility of the designed *Camellia oleifera* flower harvesting actuator, which provides a more efficient way to pick *Camellia oleifera* flowers.

Mechanized harvesting of *Camellia oleifera* flowers is an inevitable trend for the benign development of the *Camellia oleifera* industry. This research solves the current situation resulting in no mechanical picking methods for *Camellia oleifera* flowers. In the future, we will also increase the research on the mechanical picking of *Camellia oleifera* flowers to create methods for the intelligent picking of *Camellia oleifera* flowers as soon as possible.

Author Contributions: Writing—review & editing, Z.W. and L.L.; Writing—original draft, Z.W.; Project administration, Q.Z.; Methodology, Z.W.; Investigation, X.G. and J.L. All authors have read and agreed to the published version of the manuscript.

Institutional Review Board Statement: Not applicable.

Informed Consent Statement: Not applicable.

Data Availability Statement: Not applicable.

Conflicts of Interest: The authors declare no conflict of interest.

References

1. Li, S.Z.; Yao, Q.; Li, H. Functional analysis of BRLZ motif of the transcription factor CfHac1 in Colletotrichum fructicola. *J. Beijing For. Univ.* **2021**, *43*, 70–76.
2. Li, M.M.; Zhang, W.; Lv, J.M.; Shu, J.P.; Ye, B.H.; Wang, H.J. Effects of the damage caused by Curculio chinensis on fruit production of *Camellia* tree and nutritional value of *Camellia* seed oil. *Plant Prot.* **2016**, *42*, 65–68+79.
3. Wei, X.P.; Lin, P.; Wang, H.; Li, Y.; Li, H.J.; He, X.J. Pollinator diversity of *Camellia oleifera* forest and foraging behavior of dominant species under different habitat of Guizhou. *Southwest Chin. J. Agric. Sci.* **2020**, *33*, 2145–2152.
4. Hu, J.H.; Liu, F.; Qin, J.M. The recent advances in research on effective pollinators of *Camellia oleifera*. *J. Bee.* **2019**, *39*, 27–30.
5. Chen, Y.; Yuan, D.Y.; Li, K.; Yang, Y.H.; Jin, Y.J.; Lin, M.H.; Zou, F. Viability determination and preservation of pollen of *Camellia oleifera* 'Huashuo', 'Huaxin' and 'Huajin'. *Acta Agric. Univ. Jiangxiensis.* **2020**, *42*, 118–126.
6. Yang, J.; Yang, H.P.; Xie, W.; Hao, H.T.; Feng, H.Z.; Wang, L. Parameter optimization and economic analysis of unmanned aerial vehi-cle(UAV) assisted liquid pollination for Kuerlexiangli pear. *J. Fruit Sci.* **2021**, *38*, 1691–1698.
7. Karimi, H.R.; Zeraatkar, H. Effects of artificial pollination using pollen suspension spray on nut and kernel quality of pistachio cultivar owhadi. *Int. J. Fruit Sci.* **2016**, *16*, 171–181. [CrossRef]
8. Zeng, H.F. Research on Hop's Machine Pickability. Master's Thesis, Xinjiang Agricultural University, Wulumuqi, China, 2000.
9. Willoughby, R.A.; Solie, J.B.; Whitney, R.W. A mechanized harvester for marigold flowers. In Proceedings of the ASAE International Meeting, Milwaulkee, WI, USA, 9–12 July 2000.
10. Dehkordi, S.; Hanjani, P.J.; Chegini, G.R. Design, construction and evaluation of chrysanthemum flower stem cleaner machine. *Jordan J. Mech. Ind. En.* **2014**, *8*, 369–375.
11. Ravutov, S.T.; Olimjonov, R. Features of picking cotton from the spindles of a vertical-spindle cotton picker with their variable kinematic modes. *IOP Conf. Ser. Earth Environ. Sci.* **2021**, *868*, 012071. [CrossRef]
12. Wang, Y.J. Study on Picking Robots for Edible Rose. M.A. Thesis, Kunming University of Science Technology, Kunming, China, 2014.
13. Cao, W.B.; Jiao, H.B.; Liu, J.D.; Yang, S.P.; Chen, B.B.; Sun, W.L. Design of safflower filament picking device based on TRIZ theory. *Trans. Chin. Soc. Agric. Mach.* **2018**, *49*, 76–82.

14. Ji, C.Y.; Wang, C.X.; Gu, B.X.; Zhang, C. Structure design and experiment of hang-push chrysanthemum morifolium comb-teeth picking machine. *Trans. Chin. Soc. Agric. Mach.* **2016**, *47*, 143–150+142.

15. Wang, R.; Zheng, Z.; Zhu, G.; Gao, L.; Cui, B. Research status of harvesting machines for medicinal flowers. In Proceedings of the ASABE Annual International Meeting, Boston, MA, USA, 7–10 July 2019.

16. Fu, L.; Okamoto, H.; Hoshino, Y.; Esaki, Y.; Kataoka, T.; Shibata, Y. Efficient harvesting of Japanese blue honeysuckle. *Eng. Agric. Environ. Food* **2011**, *4*, 12–17. [CrossRef]

17. Qin, J.; Yin, Y.; Liu, Z.; Du, Y.; Wang, G.; Zhu, Z.; Li, Z. Optimization of maize picking mechanism by simulation analysis and high-speed video experiments. *Biosyst. Eng.* **2020**, *189*, 84–189. [CrossRef]

18. Wang, X.N.; Chen, Y.Z.; Wang, R.; Peng, S.F.; Chen, L.S.; Ma, L.; Tang, W.; Luo, J. Flowering and pollinating specifications of *Camelia oleifera* cultivars. *J. Cent. South Univ. For. Technol.* **2013**, *33*, 1–6+181.

19. Huang, X.B. Research on Ecological Cultivation Technology of *Camellia oleifera* Abel Efficiently. Master's Thesis, Zhejiang A & F University, Hangzhou, China, 2015.

20. Xu, X.W.; Yan, J.C.; Wei, H.; Bao, G.C.; Ji, L.L.; Xie, H.X. Determination of static friction coefficient of peanut pod under different moisture content. *J. Chin. Agric Mech.* **2022**, *43*, 93–97. [CrossRef]

21. Hao, L.J.; Ye, J.; Yue, G.F.; Gong, J.Y.; Li, M.S.; Zeng, B.G. A Study of the physical and mechanical properties of the shortened stem of tumorous stem mustard. *J. Southwest Univ. Nat. Sci. Ed.* **2018**, *40*, 30–36.

22. Patel, A.; Bhalani, J. Development of cotton flower picking machine based on machine vision technique. *Int. J. Adv. Comput. Sc.* **2018**, *180*, 22–26. [CrossRef]

23. Mu, L.T.; Cui, G.P.; Liu, Y.D.; Cui, Y.J.; Fu, L.S.; Yoshinori, G. Design and simulation of an integrated end-effector for picking kiwifruit by robot. *Inf. Process. Agric.* **2020**, *7*, 58–71. [CrossRef]

24. Xie, H.R. Design and Experiment of Belt Conveyor Header for Soybean Combine Harvester. Master's Thesis, Shandong University of Technology, Zibo, China, 2019.

25. Wu, X. Development of Driving and Conveying Device for Maize Harvester with Stem and Barley Harvesting. Master's Thesis, Jilin Agricultural University, Changchun, China, 2019.

26. Ding, D.; Qin, Z.Z. Investigation of the angular motion of suspended body in recovery systems. *Chin. Space Sci. Technol.* **2009**, *29*, 62–67.

27. Zhang, N.; Wang, Z.; Wang, D.L. Attitude algorithm of motion rigid body based on differential equations and acceleration. *Mach. Des. Manuf.* **2021**, *10*, 215–219+224.

28. Pan, L.B.; Li, H.; Zuo, Z.J. Kinematic analysis on the conical roll's rotation during the process of the ring's radial-axial rolling. *J. Mach. Des.* **2021**, *38*, 80–83.

29. Panou, G.; Korakitis, R. Analytical and numerical methods of converting cartesian to ellipsoidal coordinates. *J. Geod. Sci.* **2021**, *11*, 111–121. [CrossRef]

30. Wang, Z.F.; Liu, K.; Chu, F.T. On the transformation of rectan-gular coordinates in space of points on the ellipsoidal surface. *Eng. Surv. Mapp.* **2019**, *28*, 1–5.

31. Zhu, W. The relationship between angular velocity and angular momentum of rigid body in fixed point motton. *Phys. Eng.* **2016**, *26*, 31–34+39.

32. Wang, Y.; Lv, Q.S.; Liu, C.; Liu, S.X. Geometric character of euler angles describing rotation of a rigid body with one fixed point. *J. Liaoning Univ. Nat. Sci. Ed.* **2009**, *36*, 197–200.

33. Tan, Z.P.; Luo, Y.S.; Li, K. Mathematical model of micromachined vibratory wheel gyroscopes and analysis of its working state. *J. Harbin Eng. Univ.* **2002**, *23*, 33–36.

34. Amer, T.S.; Abady, I.M. Solutions of Euler's dynamic equations for the motion of a rigid body. *J. Aerospace Eng.* **2017**, *30*, 04017021. [CrossRef]

35. Cui, G.P.; Wang, J.Z.; Wen, S.T.; Wei, Y.Z.; Cui, Y.J.; Niu, Z.J. Design and test of monomer sorting and orientational conveying device for postharvest cabbage. *Trans. Chin. Soc. Agric. Mach.* **2021**, *52*, 351–360.

36. Jiang, S.; Sui, K.; Yang, D.Y.; Chen, Z.Y.; Xu, B.; Wang, G.J. Turnover motion mechanism of automatic orientation of eggs according to pointed end and blunt end. *Trans. Chin. Soc. Agric. Mach.* **2014**, *45*, 215–222.

37. Philips, C. Equations of motion for spin stabilization analysis in terms of euler angles. *Aiaa J.* **1964**, *2*, 1485–1486.

38. Kim, D.Y.; Suh, J.E.; Han, J.H.; Seo, H.; Kim, K.S. Study on a spin stabilization technique using a spin table. *J. Korean Soc. Aerona.* **2018**, *46*, 419–426.

39. Yusuppov, S.; Shoumarova, M.; Abdillayev, T.; Shovazov, K.; Xusainov, B. Quality of friction drive moving spindels of cotton picking machine with vertical spindle. *IOP Conf. Ser. Earth Environ. Sci.* **2020**, *614*, 012142.

40. Qing, R.M.; Zhi, P.H.; Jie, Q. Finite element analysis and optimal design of frictional roller. *Appl. Mech. Mater.* **2013**, *2307*, 221–224.

41. Xing, Q.Y.; Shuang, Y.Y.; Quan, Y.N. Analysis and design of the roller for belt conveyor based on ANSYS. *Adv. Mater. Res.* **2014**, *2471*, 315–319.